ChemComm

Accepted Manuscript

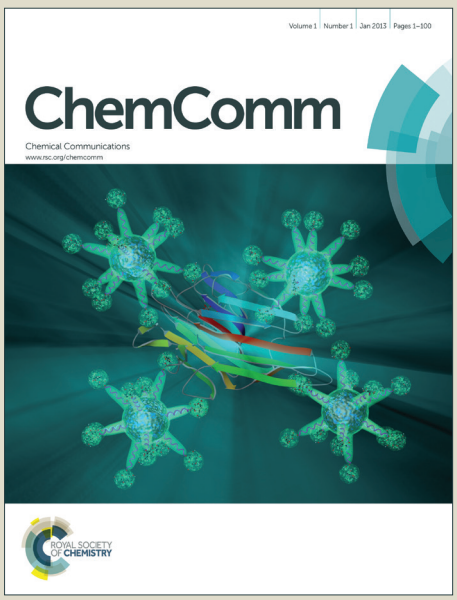

ROYAL SOCIETY OF CHEMISTRY

www.rsc.org/chemcomm

Journal Name

RSCPublishing

COMMUNICATION

Gold Nanoprobes for Detecting DNA Adducts

Cite this: DOI: 10.1039/xoxxoooooox

Ioannis A. Trantakis and Shana J. Sturla[a]

Received ooth January 2012,
Accepted ooth January 2012

DOI: 10.1039/xoxxoooooox

www.rsc.org/

A colorimetric probe for the detection of a mutagenic DNA adduct within a sequence was created. The probe involves incorporation of a synthetic nucleoside that selectively pairs opposite a target DNA adduct into oligonucleotides that are conjugated to gold nanoparticles (AuNPs).

Genotoxic chemicals covalently bind to DNA forming adducts. Their level and persistence reflect the severity of exposure and cellular susceptibility to toxicity; thus, DNA adducts can be chemical biomarkers for carcinogenesis initiation and anti-cancer drug efficacy. Their ability to induce mutations depends on their chemical structure, abundance, propensity to be recognized by DNA repair proteins, and position within the genome.[1, 2] Local DNA sequence context influences the rate of adduct formation, repair, and mispairing potency.[3] Furthermore, location within a gene determines whether mutations influence protein structure and function.

Despite the biological relevance of DNA adduct location, analysis techniques, including ^{32}P postlabeling, immunoassays, fluorescence spectroscopy, and mass spectrometry,[4] detect monomeric nucleoside or nucleotide adducts without accounting for sequence context. The emerging technique of Single Molecule Real Time sequencing (SMRT)[5] has sequence-discriminating potential, but has not been demonstrated for mixtures. We report here a strategy to sense a mutagenic alkylated DNA adduct in a sequence-specific manner and in a mixture with unmodified DNA. The basis is a novel combination of chemically modified nucleic acids and AuNPs, and the target is O^6-BenzylG (O^6-BnG, Fig. 1A), representing bulky alkyl-DNA adducts from carcinogens such as N-methylbenzylnitrosamine.[6, 7] To our knowledge, AuNPs have never been combined with non-natural DNAs for detecting DNA adducts, nor has any method for quantification of a DNA alkylation adduct in a specific sequence context within a mixture been reported.

AuNPs have exceptionally high absorption coefficients, enabling higher sensitivity than conventional dyes and fluorophores, and their plasmonic properties strongly depend on shape, size and inter-particle distance.[8, 9] Additionally, surface-enhanced Raman scattering, size enhancement by silver deposition, and high conductivity can greatly enhance signal strength.[10, 11] Thus, AuNPs as labelling tags are the basis of numerous extremely sensitive and sophisticated means to detect unmodified DNA and single nucleotide polymorphisms (SNP) in unamplified human genomic DNA samples,[10, 12-14] but there is no reported chemical basis for adapting these approaches to detect DNA adducts.

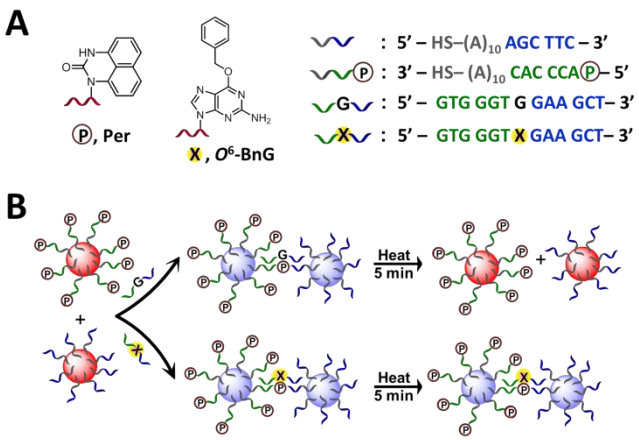

Fig. 1 A) The synthetic nucleoside Per forms stable base pairs with O^6-BnG, a bulky DNA adduct. B) AuNP probes: AuNPs tail-to-tail functionalized with two sets of oligonucleotides, with Per incorporated into one set, indicated with terminal P. Target binding leads to NP aggregation and red to purple color change. At a critical temperature, aggregates from the G-containing target disperse and the solution becomes red again while those formed from the O^6-BnG target remain aggregated and their solution appears purple.

[a]Institute of Food, Nutrition and Health, Department of Health Sciences and Technology, ETH Zurich
Email: sturlas@ethz.ch

† Electronic Supplementary Information (ESI) available: Experimental details, additional figures and tables. See DOI:

The new probes created for this study consist of AuNPs conjugated to two sets of oligonucleotides, one of which is unique in containing a perimidinone-derived nucleoside (Per, Fig. 1A) that forms a more stable base pair with O^6-BnG than with the canonical base G in a DNA duplex.[15-17] The Au-bound oligonucleotides align in a tail-to-tail fashion to form a sequence complementary to the target (Fig. 1B). In the absence of a matched target, the AuNPs remain dispersed, and the suspension has a red color. When a matched target is added, it hybridizes to the probes and brings the AuNPs together. Their close proximity causes a coupling of their individual localized plasmon fields, which induces a color change to purple. Aggregates containing adducted DNA have enhanced thermal stability due to the higher binding affinity of Per towards alkylated DNA. Thus, when the samples are heated, aggregates from undamaged targets disperse and the solution becomes red again while those from the damaged target remain aggregated and the solution appears purple.

The probes were constructed by functionalizing AuNPs (d=20 nm) with 5'-thiol-modified or 3'-thiol-modified oligonucleotides. The 5'-modified oligonucleotide is a 16-mer consisting of an $(A)_{10}$ spacer and a 6-mer recognition sequence; 3'-modified oligonucleotide is a non-conventional 17-mer consisting of an $(A)_{10}$ spacer and a 7-mer recognition sequence ending with a 5'-Per residue. The two thiolated oligonucleotides were complementary to the 5'- and 3'- ends of the 13-base target strand. The dispersed functionalized 20-nm AuNPs exhibited a characteristic surface plasmon resonance (SPR) band at 527 nm (Fig. S1). Upon AuNP aggregation (induced by the addition of target DNA) the 527-nm SPR peak decreased while absorbance in the 700-nm region increased (Fig. S1). Thus, the absorbance ratio 700 nm vs. 527 nm was used to characterize aggregation state. The test targets were 13-mer oligonucleotides containing O^6-BnG, G (Fig. 1A), or T in the position opposite Per and located at the centre of the strand to promote discrimination (Table S1).[18-20] A non-complementary 13-mer was used as a negative control (Table S1, irrelevant target).

To assess how well the system distinguished between adducted and non-damaged target strands, the magnitute of aggregation upon adding target (20 and 100 nM) was determined by UV/Vis spectrophotometry (Fig. S2). AuNP aggregation occurred in the presence of complementary targets but not for the irrelevant target. To compare aggregation rates, we calculated the times at which DNA-AuNP aggregates were 50% assembled (i.e., the hybridization transition time, T_h),[21, 22] which occurs when the absorbance ratio (A_{700}/A_{527}) reaches half its maximal value. The T_h for probe:O^6-BnG-target was 12.2 min, while the T_h for probe:G-target or probe:T-target increased to 24.9 and 47.4 min, respectively (Fig. S3).

The thermal stability of AuNP probe:target aggregates was evaluated by comparing their melting temperatures (T_m) by monitoring the 527 nm absorbance of their suspensions as a function of temperature. Increased absorbance reflects denaturation of the hybridized strands within the aggregates. The aggregates exhibited characteristic, exceptionally sharp melting transitions (Fig. 2) derived from the cooperativity of nanoparticle dissociation (the network of nanoparticles gets progressively weaker as multiple DNA linkers dissociate) and the LSPR phenomenon.[23-25]

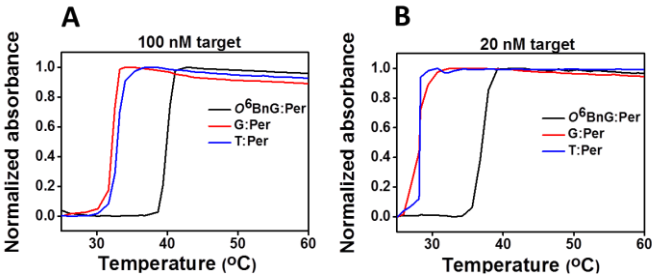

Fig. 2 Melting curves for AuNP aggregates with varying target identity and concentration. A) 100 nM or B) 20 nM O^6-BnG-, G- and T- containing 13-mer target oligonucleotides. Absorbance values at 527 nm were recorded as a function of temperature.

The T_m of the AuNP probe:O^6-BnG target aggregates (100 nM) was 39.6 °C, while those for aggregates formed from G- and T-targets (100 nM) were 33.3 and 32.7 °C, respectively (Fig. 2A, Table S2). At lower target concentrations (20 nM), the corresponding T_m values were 37.0 vs. 29.2, and 28.9 °C (Fig. 2B, Table S2). Notably, the differences between melting temperatures (ΔT_m) of aggregates formed from O^6-BnG- vs. G-containing targets remained high at both concentrations (7.8 ± 0.8 °C at 20 nM, 6.3 ± 1.0 °C at 100 nM). Due to the high sensitivity of aggregation state to temperature, we could visually distinguish target identity on the basis of the color of the aggregate solution (Fig. S4). Solutions heated above the T_m of the aggregates became red due to the dissociation of the interconnecting targets while at temperatures below the T_m, they remained purple.

The thermal stabilities of the nanoprobe aggregates containing Per paired opposite O^6-BnG, G, or T correlated with the relative thermal stabilities of the corresponding free DNA duplexes (i.e., duplexes not conjugated to nanoparticles). Thus, duplexes (2.2 μM) formed between target oligonucleotides (Table S1) and Probe 1, whose sequence combines the recognition sequences of the 5'-thiol-modified and the 3'-thiol-modified oligonucleotides, exhibited broad melting curves with T_m values of 60, 55, and 53 °C when Per was placed opposite O^6-BnG, G, or T, respectively, translating to the ability of Per to form a more stable base pair with O^6-BnG than with G (Table S3). We also tested the impact of Per on the thermal stability of DNA duplexes when O^6-BnG was not opposite Per in the recognition sequence, but one or two positions away (Table S1). The resulting DNA duplexes had lower T_m values than the corresponding DNA duplexes that contained the natural base C at the middle of the probe strand (Table S4). Thus, in that case the presence of Per in the probe strand decreased the thermal stability of the DNA duplexes. Therefore, the recognition of O^6-BnG by Per is specific to the case when they are directly paired within a DNA duplex, supporting the sequence specificity of the hybridization event that is the basis of the detection strategy.

The origin of the increased and sequence-specific thermal stability of constructs containing O^6-BnG paired with Per arises from the increased stability of this unnatural base pair. Recently, we have shown that the molecular basis by which Per distinguishes between O^6-BnG and G in a short duplex is that Per adopts a *syn* conformation and intercalates into the duplex. This orientation provides a binding pocket that allows the benzyl group of O^6-BnG to intercalate between Per and T of a 3'-neighbor A:T base pair. In contrast, when Per is placed opposite G, it adopts the *anti* conformation about the glycosyl bond and forms a less stable wobble pair with G.[26]

A major hurdle is for the increased stability of the unnatural pair between Per and O^6-BnG to render the nanoprobes diagnostic of a small amount of adducted DNA in mixtures containing undamaged DNA. Thus, we investigated whether the O^6-BnG target still increased the thermal stability of the aggregates in the presence of other targets that also induced aggregation. Solutions containing the two AuNP probes (1 nM each) and a mixture of the G, T, and irrelevant targets (100 nM each) were supplemented with either O^6-BnG target or G target, and upon aggregation, the solutions were heated for 5 min at specific temperatures ranging from 30-42 °C. The absorbance ratios A_{700}/A_{527} decreased at higher temperatures, indicating aggregate dispersion (Fig. 3A) and discrimination between the two possible complexes ($\Delta(A_{700}/A_{527})$) was maximal at 35 °C (Fig. 3B).

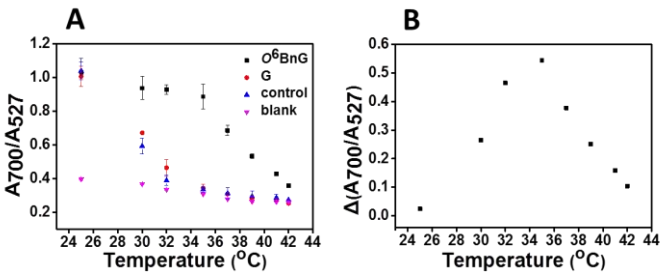

Fig. 3 A) Dependence of absorbance ratios on temperature of aggregates formed from AuNP probes (1 nM each) and target mixtures (100 nM of each G,T and irrelevant target) supplemented with either O^6-BnG- (100 nM final concentration) or G-containing targets (200 nM final concentration). An aggregate solution formed from the initial mixture (control) and a solution containing only the AuNP probes (blank) served as controls. Data is mean±SD from three independent experiments. B) Differential absorbance ratios between aggregates formed from target mixture (100 nM of each G,T and irrelevant target) supplemented with O^6-BnG-containing target (100 nM final concentration) and aggregates formed from target mixture supplemented with G-containing target (200 nM final concentration).

The remarkable discrimination for matched targets suggested a potential to relate the increase in thermal stability of aggregates, even formed in the presence of mixed targets, with O^6-BnG concentration. Thus, we supplemented G, T and irrelevant target (20 nM each) mixtures with only 2 pmol of O^6-BnG (20 nM final concentration) or G (40 nM final concentration) targets and evaluated the aggregation of AuNP probes (1 nM each). At these lower concentrations, aggregates formed from solutions supplemented with either O^6-BnG or G targets could be distinguished even at 25 °C, i.e. no heating was required (Fig. S5A). Maximum discrimination between the O^6-BnG and G targets was achieved at 29 °C ($\Delta(A_{700}/A_{527}) = 0.45$, Fig. S5B).

We further evaluated sensitivity by measuring aggregation in samples containing decreasing relative concentrations of O^6-BnG target. Solutions of aggregates containing the two AuNP probes (1 nM each) in a mixture of G, T and irrelevant targets (100 nM each) were supplemented with O^6-BnG/G target solutions (10 pmol in total) in which the relative concentration of O^6-BnG ranged from 0-10 % (Table S5). Upon aggregation, the solutions were heated for 5 min at 35 °C, the temperature at which maximum discrimination had been observed (Fig. 3B). Under these conditions, A_{700}/A_{527} values decreased linearly (R^2=0.981) as the relative concentration of O^6-BnG decreased from 10% to 0%, indicating a corresponding decrease in aggregate thermal stability.

The detection limit for alkylated DNA was 300 fmol O^6-BnG target (3 nM) in the presence of 10 pmol of G target (100 nM), or 1.3 % O^6-BnG (Fig. S6). Moreover, when the presence of other targets (T-containing and irrelevant sequences) is taken into account, the detection limit was 300 fmol O^6-BnG target (3 nM) in 40 pmol of DNA (400 nM), or 0.74 % O^6-BnG (Fig. 4). These values and the compatibility of the probes with ultrasensitive AuNP-based technologies currently used for unamplified genomic samples[13-14,27-29] support the potential for sequence-specific detection of DNA adducts in biological samples. Engineering such a real-sample application would require the materials and chemical basis established in this study implemented in the manner of common AuNP-based SNP arrays, involving digesting a known-concentration DNA sample, arrayed format of probes functionalized with different genomic sequences simultaneously, detection by scanometric,[13,27] light-scattering,[28,29] or electrical detection,[14] and possible salt washing instead of heating for mismatch discrimination.[14]

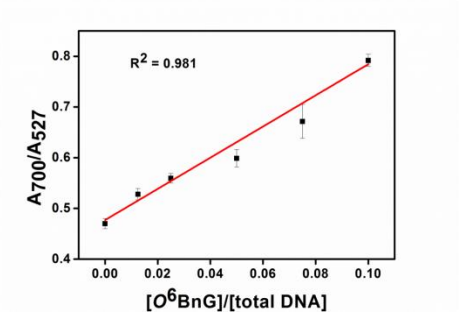

Fig. 4 Linear relationship between absorbance ratios (700/527 nm) and relative O^6-BnG target concentration ([O^6-BnG]/[total target]). Samples were heated to 35 °C for 5 min. Data points indicate mean±SD from three independent experiments.

The present study constitutes the first strategy for detecting a DNA adduct in a specific DNA sequence context within a mixture of different sequences. Specificity is derived from the molecular recognition properties of a synthetic base for a DNA adduct in a duplex, and the exceptionally sharp colorimetric

melting transitions associated with the AuNP polymeric network, allowing visual discrimination between adducted and native DNA. The new chemical principle and materials established in this study, integrated with previously well-established detection techniques, may enable in-gene monitoring of O^6-alkyl-guanine adducts as chemical biomarkers of carcinogen exposure or in vitro sensitivity assays for individualized cancer therapies, which is currently not possible.[30-32] By creating a variety of novel DNA adduct-targeting synthetic bases it can be envisioned to apply the concepts introduced here for additional adducts. To this end, the method described herein is immediately suitable tor testing altered nucleobase candidates for their adduct complementarity, as it is more sensitive than conventional DNA melting assays and reduces the required quantity of synthetic oligonucleotides.

This work was supported by the European Research Council (260341). We thank Dr. Rahul R. Lad, Claudia Otto and Arman Nilforoushan for synthesizing modified nucleosides and oligonucleotides, and Dr. Heidi Dahlmann for contributions to writing.

Notes and references

1. J. C. Delaney and J. M. Essigmann, *Biochemistry*, 2001, **40**, 14968-14975.
2. J. C. Delaney and J. M. Essigmann, *Chem. Biol.*, 1999, **6**, 743-753.
3. M. F. Denissenko, A. Pao, M. S. Tang and G. P. Pfeifer, *Science*, 1996, **274**, 430-432.
4. P. Koivisto and K. Peltonen, *Anal. Bioanal. Chem.*, 2010, **398**, 2563-2572.
5. B. A. Flusberg, D. R. Webster, J. H. Lee, K. J. Travers, E. C. Olivares, T. A. Clark, J. Korlach and S. W. Turner, *Nat. Methods*, 2010, **7**, 461-465.
6. A. K. Arrington, E. L. Heinrich, W. Lee, M. Duldulao, S. Patel, J. Sanchez, J. Garcia-Aguilar and J. Kim, *Int. J. Mol. Sci.*, 2012, **13**, 12153-12168.
7. A. Walther, E. Johnstone, C. Swanton, R. Midgley, I. Tomlinson and D. Kerr, *Nat. Rev. Cancer*, 2009, , 489-499.
8. P. K. Jain, K. S. Lee, I. H. El-Sayed and M. A. El-Sayed, *J. Phys. Chem. B*, 2006, **110**, 7238-7248.
9. N. G. Khlebtsov, L. A. Trachuk and A. G. Mel'nikov, *Opt. Spectrosc.*, 2005, **98**, 77-83.
10. Y. W. C. Cao, R. C. Jin and C. A. Mirkin, *Science*, 2002, **297**, 1536-1540.
11. P. Baptista, E. Pereira, P. Eaton, G. Doria, A. Miranda, I. Gomes, P. Quaresma and R. Franco, *Anal. Bioanal. Chem.*, 2008, **391**, 943-950.
12. X. Cao, Y. Ye and S. Liu, *Anal. Biochem.*, 2011, **417**, 1-16.
13. Y. P. Bao, M. Huber, T. F. Wei, S. S. Marla, J. J. Storhoff and U. R. Muller, *Nucleic Acids Res.*, 2005, **33**, e15.
14. S.-J. Park, T. A. Taton and C. A. Mirkin, *Science*, 2002, **295**, 1503-1506.
15. J. C. Gong and S. J. Sturla, *J. Am. Chem. Soc.*, 2007, **129**, 4882-4883.
16. H. L. Gahlon and S. J. Sturla, *Chem. - Eur. J.*, 2013, **19**, 11062-11067.
17. T. Angelov, H. A. Dahlmann and S. J. Sturla, *Bioorg. Med. Chem.*, 2013, **21**, 6212-6216.
18. F. Huber, H. P. Lang, N. Backmann, D. Rimoldi and C. Gerber, *Nat. Nanotechnol.*, 2013, **8**, 125-129.
19. G. Doria, B. G. Baumgartner, R. Franco and P. V. Baptista, *Colloids Surf., B*, 2010, **77**, 122-124.
20. D. Y. Zhang, S. X. Chen and P. Yin, *Nat. Chem.*, 2012, **4**, 208-214.
21. I. A. Trantakis, S. Bolisetty, R. Mezzenga and S. J. Sturla, *Langmuir*, 2013, **29**, 10824-10830.
22. J.-H. Oh and J.-S. Lee, *Anal. Chem.*, 2011, **83**, 7364-7370.
23. R. Elghanian, J. J. Storhoff, R. C. Mucic, R. L. Letsinger and C.A.Mirkin, *Science*, 1997, **277**, 1078-1081.
24. J. J. Storhoff, R. Elghanian, R. C. Mucic, C. A. Mirkin and R. L. Letsinger, *J. Am. Chem. Soc.*, 1998, **120**, 1959-1964.
25. J. J. Storhoff, A. A. Lazarides, R. C. Mucic, C. A. Mirkin, R. L. Letsinger and G. C. Schatz, *J. Am. Chem. Soc.*, 2000, **122**, 4640-4650.
26. E. A. Kowal, R. R. Lad, P. S. Pallan, E. Dhummakupt, Z. Wawrzak, M. Egli, S. J. Sturla and M. P. Stone, *Nucleic Acids Res.*, 2013, **41**, 7566-7576.
27. T.A. Taton, C.A. Mirkin, R.L. Letsinger, *Science*, 2000, **289 (5485)**, 1757-1760.
28. J.J. Storhoff, A. D. Lucas, V. Garimella, Y. P. Bao, U. R. Müller, *Nature Biotechnology*, 2004, **22**, 883 - 887.
29. J. J. Storhoff, S. S. Marla, Y. P. Bao, S. Hagenow, H. Mehta, A. Lucas, V. Garimella, T. Patno, W. Buckingham, W. Cork, U. R. Müller, *Biosensors and Bioelectronics*, 2004, **19**, 875–883.
30. M. Otteneder and W. K. Lutz, *Mutat. Res., Fundam. Mol. Mech. Mutagen.*, 1999, **424**, 237-247.
31. C. P. Wild, *Mutagenesis*, 2009, **24**, 117-125.
32. B. Kaina, G. Margison and M. Christmann, *Cell. Mol. Life Sci.*, 2010, **67**, 3663-3681.

